

# Thermodynamic processes of Si-interstitial clusters

Jeongnim Kim,<sup>1</sup> Stefan Birner,<sup>1,2</sup> David A. Richie,<sup>1</sup> John W. Wilkins<sup>1</sup> and Arthur F. Voter<sup>3</sup>

<sup>1</sup>Department of Physics, Ohio State University, Columbus, OH, USA

<sup>2</sup>Walter Schottky Institute, TU Munich, Am Coulombwall 3, D-85748 Garching, Germany

<sup>3</sup>Theoretical Division, Los Alamos National Laboratory, Los Alamos, NM, USA

## ABSTRACT

Structural and dynamical properties of silicon interstitial defects are extracted from extensive atomistic simulations using *ab initio* total energy calculations. With increasing number of interstitials, the stable defect shape evolves from compact to chain-like to rod-like. The rod-like  $\{311\}$  defect, formed from  $(011)$  interstitial chains, is stabilized as it grows, elongating in the chain direction. We utilize new accelerated dynamics algorithms based on the parallel-replica method and reliable empirical potentials to efficiently explore large configurational space involving many degrees of freedom. We evaluate the empirical potentials that have been widely used for bulk silicon in light of the energetic and structural properties of interstitial defects.

**Keywords:** silicon, interstitial, defects, potentials, simulations.

## 1 Introduction

Interstitial defects control the dopant diffusion in ion-implanted silicon by providing traps for and sources of mobile interstitials [1]–[4]. For example, boron transient enhanced diffusion (B-TED) in ion-implanted samples is the limiting factor in shallow-junction fabrication of submicron Si-based devices. Extensive experimental work established that B-TED persists under interstitial supersaturation conditions as in ion-implanted samples during rapid thermal annealing steps [1], [2]. A class of extended  $\{311\}$  defects is linked to the source of B-TED by providing mobile interstitials stored in the defects. On the other hand, smaller interstitial clusters that are dissolved at lower energy cost are claimed to be responsible for B-TED under low-energy ion-implantation conditions [3].

Traditionally, B-TED has been modeled by solving coupled diffusion equations with the governing cluster kinetics determined by the diffusion properties of mobile interstitials and the nucleation properties of mobile interstitials to existing interstitial traps [4], [5]. In particular, key quantities for accurate macroscopic modeling are the energies released upon an interstitial-capture by and the effective capture radii from possible interstitial-trap nuclei. Many efforts have been devoted to quantify

the energetics of the interstitial clusters [4], [6]–[12]. Recently, Cowern *et al.* reported the formation energy of interstitial clusters determined directly from TED measurements using B-doped markers by “inverse modeling of the ripening process” [4]. This approach relies on the very same assumptions needed in B-TED modeling based on kinetic Monte Carlo method [5].

Alternatively, simulations using interatomic potentials probe the energetically and kinetically important processes for B-TED at the atomistic level [6]–[12]. Recent advances in numerical algorithms for quantum and classical molecular dynamics simulations and growing computational power have expanded the length and time scales that can be explored by atomistic simulations [13], [14].

We summarize the thermodynamic properties of interstitial clusters obtained from extensive atomistic simulations using a wide range of interatomic potentials, from classical to *ab initio* potentials. Parallel-replica simulations [14] using a classical modified embedded atom (MEAM) potential [15] probe the microscopic processes of cluster growth via interstitial-diffusion and interstitial-nucleation. The local minimum configurations and transition paths captured by parallel-replica simulations are used as the inputs for *ab initio* total energy calculations. A quantitative growth model for interstitial defects from isolated interstitials to extended  $\{311\}$  defects is derived from the *ab initio* energetics.

## 2 Growth of Si-interstitial clusters

Figure 1 presents the stability trends of interstitial clusters predicted by *ab initio* total energy calculations within the local density approximation (LDA) [10] compared with the inverse modeling [4]. In general, the stability of interstitial clusters increases as the size  $n$  increases. We find that the stable configuration for a given size can be (a) **compact** for small clusters, (b) **elongated** for medium clusters and (c) **planar** for large clusters. Amongst many local minimum configurations captured by parallel-replica runs, the two solid lines connect the formation energies of the most stable structures for the compact and elongated classes [10]. The formation energies extracted from the inverse modeling qualitatively agree with those calculated by *ab initio* sim-

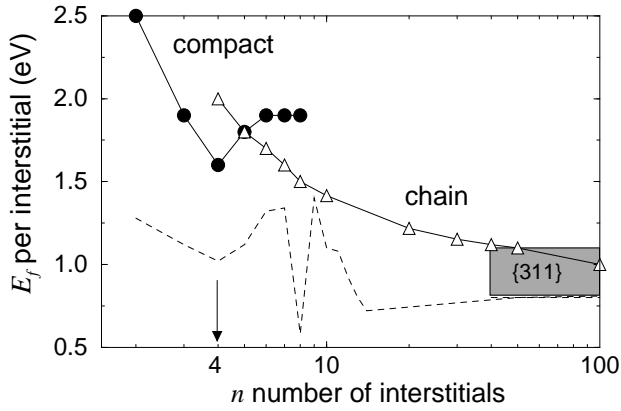


Figure 1: Formation energies  $E_f$  per interstitial of  $n$ -interstitial clusters. Symbols  $\bullet$  and  $\triangle$  denote *ab initio* LDA results. *Ab initio* LDA calculations imply that the transition from the compact to elongated shape would occur at  $n \sim 5$ . The dashed line is the formation energy trend predicted by the inverse modeling of Cowern *et al.* [4]. Our search for local minimum configurations of interstitial clusters does not find the global minimum of  $I_8$  predicted in Ref. [4].

ulations: i) interstitial defects become more stable as more interstitials are incorporated into a cluster; and ii) the formation energy converges to 0.8 eV at the large  $n$  limit in agreement with experiments [2]. The main discrepancy is found at  $n=8$ : the global minimum predicted from the inverse modeling [4] is not present in our calculations. Common elements of the ground energy configurations for small compact clusters are  $\langle 110 \rangle$  interstitialcies as shown in Fig. 2. A class of extended defects composed of elongated chains becomes energetically favorable to the compact shape as the cluster becomes larger.

Both the inverse modeling [4] and *ab initio* simulations [10] predict that the  $I_4$  cluster would be extremely stable. Several theoretical calculations proposed the compact  $I_4$  defect of  $D_{2d}$  symmetry as the ground configuration [9]–[11]. The calculated formation energy is very low at  $E_f=1.5$  eV per interstitial [10]. That all the atoms constituting the  $I_4-D_{2d}$  cluster are fully four-fold coordinated contributes to its stability. The  $I_4-D_{2d}$  structure is open, surrounded by eight seven-member rings. Accordingly, up-to four interstitials can be nucleated to form compact clusters of  $n=5-8$ . Our calculations find that compact clusters larger than  $n=8$  are unstable, with a negative interstitial-binding energy.

On the other hand, an elongated cluster can grow indefinitely by maximizing the ratio of fully four-coordinated atoms to the number of interstitials incorporated into the chain [7], [10]. The formation energy per interstitial decreases monotonically for larger chains. Assuming an interstitial capture at the chain ends, the interstitial-binding energy to the chain is  $E_b \sim 2.3$  eV. Formations

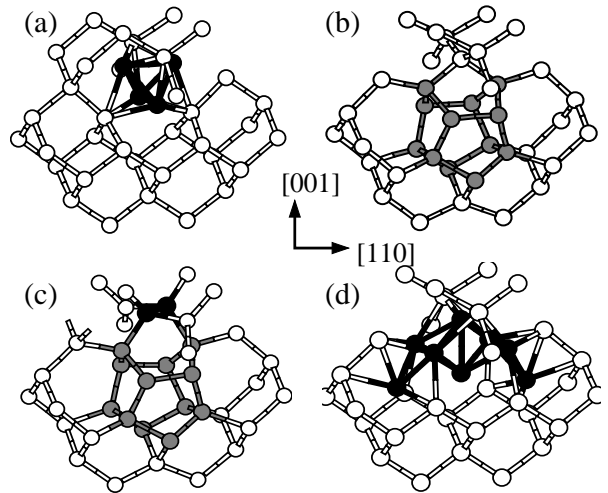


Figure 2: Core structures of compact (a)  $I_3-D_{2d}$ , (b)  $I_4-D_{2d}$ , (c)  $I_5-C_2$  and (d)  $I_5-C_{2v}$  clusters extracted from collective trajectories of parallel-replica simulations using classical MEAM potential. Within *ab initio* LDA/GGA calculations, (a)-(c) are the lowest-energy configurations for the given size. Structure (d) is a local minimum configuration which was related to the shape transition in Ref. [12].

of elongated clusters can further lead to the growth of “rod-like”  $\{311\}$  defects. Indeed, the atomic structure of rod-like  $\{311\}$  defects can be well described by condensations of elongated chains in the  $\{311\}$  planes in accordance with TED measurements [6]. The gray region of Fig. 1 indicates the range of formation energies of  $\{311\}$  defects for  $n > 40$  depending upon the width-to-length ratio [10].

That the structure of small clusters is fundamentally different from extended  $\{311\}$  defects was suggested by recent optical [16] and electronic [17] measurements of Si-implanted silicon exhibiting drastic changes depending upon the flux and annealing temperature. Energetically, the possible morphological transition from the point-like (compact) to extended (elongated/planar) can occur at  $n \sim 5$ . Tight-binding calculations by Bongiorno *et al.* [12] proposed a shape transition mechanism involving the  $I_5$  cluster of Fig. 2(d). Our calculations find that this structure is unstable against the lower-energy configurations modeled as an interstitial capture by the  $I_4-D_{2d}$  cluster. The negative interstitial-binding energy to a compact  $I_8$  suggests that no compact clusters of  $n > 8$  can be formed by an interstitial-nucleation process. On the other hand, elongated clusters will evolve into larger clusters by capturing available interstitials. Since interstitial-binding energies to extended defects are always positive, the growth of  $\{311\}$  defects will be only limited by the influx of mobile interstitials. However,

it is still an open question whether the shape transition from the compact to extended defect at  $n \sim 5$  is kinetically accessible.

The energetics summarized in Fig. 1 suggests the growth path: stable interstitial clusters grow by adding more interstitials. However, only a limited understanding of the critical steps leading to the cluster growth is available. In order to directly probe the microscopic processes of interstitial-diffusion and interstitial-nucleation mechanisms responsible for the defect growth, we perform extensive parallel-replica simulations using the classical MEAM potential. As predicted by previous calculations [10], [18], both single interstitial  $I_1$  and di-interstitial  $I_2$  defects are found to be mobile and diffuse by random jumps between local minima.

All interstitial clusters are efficient traps for mobile interstitial and di-interstitial defects. With an existing interstitial cluster providing a capture nucleus, the cluster growth occurs by (i) interstitial capture at the cluster boundaries and (ii) subsequent local rearrangements of the core atoms to lower-energy structures. The shape of the final cluster retains the shape of the initial cluster. For instance, when an interstitial is trapped by a metastable chain, the captured interstitial diffuses in the chain direction and eventually settles at the chain ends.

### 3 Survey of empirical potentials for interstitial defects

The energetics of Fig. 1 provides a road map for interstitial cluster growth: existing interstitial defects trap mobile interstitials to become more stable, extended defects. This interstitial-nucleation mechanism for the growth is the basic assumption for kinetic Monte Carlo simulations which have been successfully applied to model B-TED [5]. Kinetic Monte Carlo simulations rely on accurate parameterization of energies associated with the processes. Indeed, the inverse modeling by Cowern *et al.* fitted the formation energies to the secondary-ion mass spectroscopic measurements of boron profiles based on the interstitial-nucleation mechanisms [4]. Total energy calculations using *ab initio* potentials can quantify the formation energies with respect to the size without introducing fitting parameters. However, identifying the ground and local minimum structures relevant to the growth becomes computationally prohibitive as the degrees of freedom increase.

Empirical classical and tight-binding potentials provide computationally efficient alternatives for *ab initio* simulations. In recent years, steady improvement of empirical potentials for silicon has been made by several groups [15], [19]–[22]. These empirical potentials have been widely applied to simulate complicated systems, such as interstitial defects [7], [12] and dislocations [23]. Further, new algorithms for large-scale and long-time

	LDA	SW	EDIP	MEAM	TB <sub>1</sub>	TB <sub>2</sub>
$I_2$ - $C_{1h}^a$	2.5	3.1	2.8	2.1	2.8	2.5
$I_3$ - $D_{2d}^a$	1.9	2.7	3.2	2.1	2.6	2.2
$I_3$ - $C_{3v}$	2.2	3.6	3.7	1.9	2.4	3.5
$I_4^b$	1.5	2.4	2.4	1.4	2.1	2.4
$I_5$ - $C_2^c$	1.7	2.8	2.5	1.7	2.4	3.0
$I_5$ - $C_{2v}^d$	1.9	2.4	2.5	1.9	2.6	2.4
$I_5^{chain}$	1.8	2.5	2.4	1.7	2.4	2.8
$I_\infty^{chain}$	1.0	1.9	1.9	1.1	1.6	1.8

Table 1: Formation energies per interstitial obtained by *ab initio* and empirical potentials: **SW** Stillinger-Weber potential [19]; **EDIP** environment dependent interatomic potential [20]; **MEAM** classical potential in Modified Embedded Atom Method [15]; **TB<sub>1</sub>** parameters by Lenosky *et al.* [21]; and **TB<sub>2</sub>** parameters by Kwon *et al.* [22]. The symmetry symbols are specified for small clusters. Periodic boundary conditions are applied to model interstitial chains  $I_\infty^{chain}$ . The structures of compact clusters specified by superscripts (a)-(d) are shown in Fig. 2.

simulations [14] using empirical potentials offer a direct, practical means to probe the critical steps leading to cluster growth.

Reliable empirical potentials are invaluable tools to bridge the gap between *ab initio* calculations and macroscopic modeling tools. For instance, parallel-replica simulations using the classical MEAM potential reveal many local minimum configurations for  $I_5$  that have not been considered previously. Note that *ab initio* simulations appropriate to the time scale of  $I$ -diffusion and  $I$ -nucleation processes would take ten years on state-of-art parallel computers. The local minimum configurations and transition paths identified by empirical simulations are then used for accurate estimations of their formation energies and activation energy barriers by *ab initio* structural minimizations. Finally, improved qualitative and quantitative understanding of the critical microscopic processes enhances the predictions of Monte Carlo simulations at the macroscopic scale.

Table 1 presents the formation energies of selected interstitial-defect structures by several empirical potentials in comparison with the *ab initio* results. These potentials have been widely used to study properties of bulk silicon, and in particular, defects in silicon. All these potentials give the stability trends of interstitial clusters predicted by *ab initio* calculations: the energetically favorable shape evolves from the compact to elongated and eventually “rod-like”  $\{311\}$  defects.

The formation energies by the classical MEAM potential show the best quantitative agreement with the *ab initio* results. Classical potentials SW and EDIP and Kwon-TB tend to overestimate the energy of metastable structures, *e.g.*, these potentials find that the  $I_3$ - $C_{3v}$  cluster is unstable against *isolated* interstitials. For the interstitial diffusion and structural transitions between

local minima, they also tend to give too large activation energies [24] which can be attributed to the fitting steps based on only equilibrium properties. It is noteworthy that all empirical potentials find the compact  $I_4$ - $D_{2d}$  structure as the ground configuration. All the atoms of the  $I_4$ - $D_{2d}$  defect are fully four-fold coordinated with minimum bond-angle distortions from the ideal tetrahedral bonding in crystalline silicon.

As shown in Table I, many competing local minimum structures can coexist for a given size. Although the absolute formation energies are well reproduced by the MEAM potential, the relative energetics of different local minima is not always predicted correctly. The classical MEAM potential tends to favor compact structures at intermediate sizes  $n=5$ -20, inconsistent with the *ab initio* prediction that elongated clusters would become energetically more stable at  $n > 5$ . Overall, the relative stabilities are well described by the Lenosky-TB potential [21]. Most importantly, the Lenosky-TB potential accurately reproduces the small energy differences between the local minima for  $n=5$  at which the shape change is predicted to occur.

## 4 Conclusions

We summarize the energetics of interstitial clusters extracted from extensive atomistic simulations. *Ab initio* total energy calculations quantify the formation energies of many local minimum configurations obtained by parallel-replica simulations using the classical MEAM potential. The stability trends of interstitial clusters predict that the energetically favorable shape evolves from compact to elongated and eventually “rod-like” {311} defects. Steady improvement of empirical potentials for silicon in combination with new algorithms reaching to the nsec to  $\mu$ sec time scales offer exciting opportunities to directly probe the critical steps of interstitial cluster growth.

This work is supported by SRC and DOE and computational support is provided by OSC, NCSA and NERSC. Work at Los Alamos National Laboratory was performed under United States Department of Energy (DOE) contract number W-7405-ENG-36, with support from the DOE Office of Basic Energy Sciences, Division of Materials Science.

## REFERENCES

[1] D. J. Eaglesham, P. A. Stolk, H.-J. Gossmann, and J. M. Poate, *Appl. Phys. Lett.* **65**, 2305 (1994).  
 [2] P. A. Stolk *et al.*, *J. Appl. Phys.* **81**, 6031 (1997).  
 [3] L. H. Zhang, K. S. Jones, P. H. Chi, and D. S. Simons, *Appl. Phys. Lett.* **67**, 2025 (1995).  
 [4] N. E. B. Cowern, G. Mannino, P. A. Stolk, F. Roozeboom, H. G. A. Huizing, J. G. M. van

Berkum, F. Cristiano, A. Claverie, and M. Jaraíz, *Phys. Rev. Lett.* **82**, 4460 (1999).  
 [5] M. Jaraíz, G. H. Gilmer, J. M. Poate and T. D. de la Rubia, *Appl. Phys. Lett.* **68**, 409 (1996).  
 [6] S. Takeda, *Jpn. J. Appl. Phys.* **30**, L639 (1991); M. Kohyama and S. Takeda, *Phys. Rev. B* **46**, 12305 (1992).  
 [7] J. Kim, W. W. Wilkins, F. S. Khan, and A. Canning, *Phys. Rev. B* **55**, 16186 (1997).  
 [8] J. Kim *et al.*, *Phys. Rev. Lett.* **83**, 1990 (1999).  
 [9] N. Arai, S. Takeda, and M. Kohyama, *Phys. Rev. Lett.*, **78**, 4265 (1997).  
 [10] J. Kim, F. Kirchhoff, J. W. Wilkins, and F. S. Khan, *Phys. Rev. Lett.* **84**, 503 (2000).  
 [11] B. J. Coomer *et al.*, *J. Phys. Condens. Matter.* **13**, L1 (2001).  
 [12] A. Bongiorno, L. Colombo, F. Cargnoni, C. Gatti and M. Rosati, *Euro. Phys. Lett.* **50**, 608 (2000).  
 [13] G. Kresse and J. Furthmüller, *Phys. Rev. B* **55**, 11 169 (1996) and references therein.  
 [14] A. F. Voter, *Phys. Rev. B* **57**, R13985 (1998).  
 [15] T. J. Lenosky *et al.*, *Model. Simul. Mater. Sci. Eng.* **8**, 825 (2000).  
 [16] S. Coffa, S. Libertino and C. Spinella, *Appl. Phys. Lett.* **76**, 321 (2000).  
 [17] J. L. Benton *et al.*, *J. Appl. Phys.* **82**, 120 (1997); J. L. Benton *et al. ibid* **84**, 4749 (1998).  
 [18] R. J. Needs, *J. Phys.: Condens. Matter*, **11**, 10437 (1999).  
 [19] F. H. Stillinger and T. A. Weber, *Phys. Rev. B* **31**, 5262 (1985).  
 [20] M. Z. Bazant, E. Kaxiras, and J. F. Justo, *Phys. Rev. B* **56** 8542 (1997); *ibid*, **58** 2539 (1998).  
 [21] T. Lenosky *et al.*, *Phys. Rev. B* **55** 1528 (1997).  
 [22] I. Kwon, R. Biswas, C. Z. Wang, K. M. Ho and C. M. Soukoulis, *Phys. Rev. B* **49**, 7242 (1994).  
 [23] C. Wei, V. Bulatov, J. F. Justo, A. S. Argon and S. Yip, *Phys. Rev. Lett.* **84** 3346 (2000).  
 [24] M. Tang, L. Colombo, J. Zhu and T. D. de la Rubia, *Phys. Rev. B* **55**, 14279 (1997).